Toxicology in Vitro 24 (2010) 1953–1961

Contents lists available at ScienceDirect

Toxicology in Vitro

journal homepage: www.elsevier.com/locate/toxinvit

# Zinc oxide nanoparticle disruption of store-operated calcium entry in a muscarinic receptor signaling pathway

Hsiu-Jen Wang, Anna C. Growcock, Tso-hao Tang, Jennifer O'Hara, Yue-wern Huang, Robert S. Aronstam *

*Department of Biological Sciences, Missouri University of Science and Technology, Rolla, MO 65409, USA*

ARTICLE INFO

*Article history:*
Received 9 June 2010
Accepted 6 August 2010
Available online 12 August 2010

*Keywords:*
Muscarinic acetylcholine receptor
Store-operated calcium entry (SOCE)
Phospholipase Cβ
Inositol trisphosphate (IP3)
Calcium signaling
Nanoparticles toxicity
IP3
Inositol trisphophate

ABSTRACT

The influences of ZnO nanoparticles on cellular responses to activation of muscarinic receptors were studied in Chinese hamster ovary cells expressing the human M3 muscarinic acetylcholine receptor. ZnO particles (20 nm) induced cytotoxicity in a time and concentration-dependent manner: following a 24 h exposure, toxicity was minimal at concentrations below 20 μg/ml but virtually complete at concentrations above 28 μg/ml. ZnO particles did not affect antagonist binding to M3 receptors or allosteric ligand effects, but increased agonist binding affinity while eliminating guanine nucleotide sensitivity. At a noncytotoxic concentration (10 μg/ml), ZnO increased resting $[Ca^{2+}]_i$ from 40 to 130 nM without compromising calcium homeostatic mechanisms. ZnO particles had minimal effects on IP3- or thapsigargin-mediated release of intracellular calcium from the endoplasmic reticulum, but strongly inhibited store-operated calcium entry (capacitive calcium entry). The latter effect was seen as (1) a decrease in the plateau phase of the response and (2) a decrease in $Ca^{2+}$ entry upon introduction of calcium to the extracellular medium following thapsigargin-induced depletion of calcium from the endoplasmic reticulum (EC50's ≈ 2 μg/ml). Thus, ZnO nanoparticles interfere with two specific aspects of the M3 signaling pathway, agonist binding and store-operated calcium entry.



## 1. Introduction

Nanomaterials (materials that have at least one dimension in the range of 1–100 nm) are widely used in as the production of cosmetic products, transparent conductive paints and filters. Unintended exposure to nanomaterials may occur with occupational workers and end product users through inhalation, dermal absorption, or gastrointestinal tract absorption. The adverse effects of nanomaterials of various sizes and compositions on human health is being addressed (e.g., Braydich-Stolle et al., 2005; Gurr et al., 2005; Jeng and Swanson, 2006; Lewinski et al., 2008 ; Lin et al., 2006a,b, 2008; Moller et al., 2005; Timblin et al., 2002).

ZnO nanoparticles are used as catalysts and as a component of paints, wave filters, UV detectors, transparent conductive films, varistors, gas sensing monitors, solar cells, sunscreens, and other cosmetic products (Bae and Seo, 2004; Bai et al., 2003; Comini et al., 2002; Ding and Wang, 2004; Huang et al., 2006; Ramakrishna and HGhosh, 2003; Zhu et al., 2005). Inhalation of ZnO compromises pulmonary function in pigs and causes pulmonary impairment and metal fume fever in humans (Beckett et al., 2005; Fine et al., 1997).

We have recently documented the cytotoxicity of nano- and micro-size ZnO particles in cultured human bronchoaveolar carcinoma-derived cells (A549) (Lin et al., 2006a) and human bronchial epithelial cells (BEAS-2B) (Huang et al., 2009; Lin et al., 2008). This toxicity is associated with elevated oxidative stress (OS), oxidative DNA damage, and the up-regulation of several genes involved in oxidative stress responses and apoptosis. ZnO toxicity is mitigated by treatment with the antioxidant *N*-acetylcysteine. ZnO exposure also causes an increase in resting intracellular calcium levels in human bronchial epithelial cells (Huang et al., 2009).

Particles in both the nano- and micrometer range damage the olfactory bulb, disrupt the blood brain barrier, and gain entry to the central nervous system (Calderon-Garciduenas et al., 2002, 2001; Elder et al., 2006; Sharma and Sharma, 2007; Veronesi et al., 2005). The purpose of this research was to determine the extent to which ZnO nanoparticles disrupt synaptic signaling processes in a model system, M3 muscarinic receptors expressed in

*Abbreviations:* SOCE, store-operated calcium entry; CHO, Chinese hamster ovary; [$^3$H]MS, [$^3$H]*N*-methylscopolamine; PLCβ, Phospholipase Cβ; SERCA, sarco/endoplasmic reticulum ATPase; ER, endoplasmic reticulum; MTS, 3-(4,5-dimethylthiazol-2-yl)-5-(3-carboxymethoxyphenyl)-2-(4-sulfophenyl)-2H-tetrazolium; Gpp(NH)p, 5′-guanylyl-imidodiphosphate; BSS, basal salt solution.

* Corresponding author. Address: Department of Biological Sciences, Missouri University of Science and Technology, 400W 11th St., Rolla, MO 65409 USA. Tel.: +1 573 341 4819; fax: +1 573 341 4821.

*E-mail address:* aronstam@mst.edu (R.S. Aronstam).

0887-2333/$ - see front matter © 2010 Elsevier Ltd. All rights reserved.
doi:10.1016/j.tiv.2010.08.005

Chinese hamster ovary (CHO) cells. Ion channels and synaptic signaling macromolecules are particularly susceptible to toxicological agents, reflecting their exposed positions.

M3 receptors activate Gαq transducer proteins that stimulate phospholipase Cβ (PLCβ) (Aronstam and Patil, 2009). PLCβ hydrolyzes phosphatidylinositol 4,5-bisphosphate, releasing two second messengers, diacylglycerol and inositol trisphosphate (IP3). IP3 binds to the IP3 receptor on the endoplasmic reticulum (ER) to release calcium into the cytosol. Sensors in STIM1 proteins that are components of ER membranes detect the depletion of calcium in the ER. STIM1 proteins thus activated interact with Orai channel proteins in the plasma membrane to stimulate the entry of extracellular calcium, i.e., the store-operated calcium entry (SOCE) (Putney, 2009; Smyth et al., 2008).

In the present study, the influences of ZnO on M3-mediated signaling were determined at the levels of (1) receptor binding, activation and G protein coupling, (2) calcium mobilization from the endoplasmic reticulum, and (3) extracellular calcium entry. The results demonstrate minimal effects of proximal receptor events or calcium release from the endoplasmic reticulum, but a robust and specific inhibitory effect on store-operated calcium entry.

## 2. Materials and methods

### 2.1. ZnO nanoparticles

Twenty nanometer ZnO particles at >99% purity were purchased from Nanostructured and Amorphous Materials (Los Alamos, New Mexico, USA). Particle morphology, size, crystallinity, purity and agglomeration states were ascertained by scanning electron microscopy, transmission electron microscopy, inductively-coupled plasma-mass spectrometry, and X-ray diffractometry as previously reported (Huang et al., 2009). To reduce experimental variability and improve accuracy, ZnO particles were dried in a desiccator at 100 °C for 16 h before being weighed on an analytical balance. A stock suspension of 100 μg/ml ZnO was prepared in cell culture medium, and various concentrations were achieved by serial dilution.

### 2.2. Cell culture and cytotoxicity measurements

CHO cells stably transfected with a cDNA clone (in pcDNA3.1+; Invitrogen) of the human M3 muscarinic acetylcholine receptor open reading frame (cDNA Resource Center, www.cdna.org) were cultured in DME/F12 media containing 10% FCS and penicillin/streptomycin (100 IU/100 μg/ml) at 37 °C in a 5% $CO_2$ humidified environment. Cell viability was determined using the MTS reduction assay (3-(4,5-dimethylthiazol-2-yl)-5-(3-carboxymethoxyphenyl)-2-(4-sulfophenyl)-2H-tetrazolium, inner salt; Promega, Madison). Approximately 7000 cells were seeded into each well of a 96-well plate and incubated for 16 h before being exposed to ZnO for 1, 3 or 24 h.

### 2.3. Muscarinic receptor binding

[$^3$H]N-methylscopolamine ([$^3$H]MS; Perkin–Elmer), a non-selective antagonist, was used to label muscarinic receptors. CHO-M3 cells were homogenized in 50 mM Tris–HCl (pH 7.4), and an aliquot (15–30 μg protein) was incubated in the presence of [$^3$H]MS and 50 mM Tris–HCl (pH 7.4) for 60 min at room temperature in a final volume of 1 ml. In some experiments, the cells were exposed to ZnO nanoparticles for 5 h before harvesting. Binding was determined by filtration of the homogenized cells through glass fiber filters (1 μm pore size), followed by measurement of the radioactivity trapped on the filters by liquid scintillation counting. Non-specific binding was determined by including 10 μM unlabelled atropine in the incubation media.

[$^3$H]MS binding parameters (receptor concentration, dissociation constant, dissociation rate constant) were determined by nonlinear regression (DeltaGraph) using a model incorporating a single population of independent binding sites. Parameters were averaged from 3–5 independent experiments. Agonist binding affinity was determined in competition studies using carbamylcholine and 0.3 nM [$^3$H]MS. In some experiments, a guanine nucleotide (5′-guanylyl-imidodiphosphate; Gpp(NH)p) was included in the binding medium to assess receptor coupling to transducer G proteins.

### 2.4. Measurement of intracellular calcium

The concentration of intracellular calcium ($[Ca^{2+}]_i$) was monitored using the calcium-sensitive fluorescent dye, fura-2 (Molecular Probes) in a ratiometric assay. Cells (25,000) were seeded onto 35 mm glass bottom dishes and incubated for 16 h. The cells were then incubated with fura-2AM for 30 min at room temperature in a basal salt solution (BSS) comprised of 130 mM NaCl, 5.4 mM KCl, 5.5 mM glucose, 2 mM $CaCl_2$, 1 mM $MgCl_2$, and 20 mM HEPES, at pH 7.4. The cells were washed twice with fresh BSS, and the incubation continued for an additional 30 min. In "acute exposure" experiments, the ZnO nanoparticles were added at this point.

$[Ca^{2+}]_i$ was determined using an InCyt Basic IM™ Fluorescence Imaging System (Intracellular Imaging, Inc., Cincinnati, OH) at ambient temperature. The ratio of fluorescence intensities measured at 512 nm after excitation at 340 and 380 nm reflected $[Ca^{2+}]_i$. Signals from 18–25 cells were measured in each plate. Cells in which the resting $[Ca^{2+}]_i$ was not maintained within 10 nM of the average resting level were excluded from analysis, as well as cells that failed to respond to a muscarinic agonist (typically 2–3 cells/plate).

### 2.5. Statistical analysis

Parameters (calcium concentrations, dissociation constants; kinetic constants, receptor concentrations, IC50's) were compared as the means from 3–20 independent experiments (with 3 replicates in each binding measurement protocol and up to 24 replicates in each calcium measurement protocol) using Student's *t*-test. A significant difference was indicated by a $p$ value of $<0.05$. Binding parameters were determined by nonlinear regression of the binding measurement to a model incorporating a single population of non-interacting binding sites, performed using DeltaGraph 5 software.

## 3. Results

### 3.1. Muscarinic receptor mediation of cellular calcium responses

The resting cytosolic calcium concentration of CHO-M3 cells in BSS typically ranged from 33 to 54 nM (Fig. 1). Stimulation with the muscarinic agonist carbamylcholine (10 μM) led to a rapid and sustained increase in cytosolic calcium to a concentration that ranged from 500 to 700 nM (Fig. 1). CHO cells not transfected with the M3 receptor gene did not respond to carbamylcholine, and the response to carbamylcholine was completely blocked by including 10 μM atropine (a receptor antagonist) in the medium. These findings demonstrate that the response is mediated by the introduced M3 muscarinic receptor. The threshold concentration for elicitation of a response to carbamylcholine was approximately 0.3 μM.

When calcium was excluded from the extracellular medium, the initial response remained intact, but the increase in cytosolic

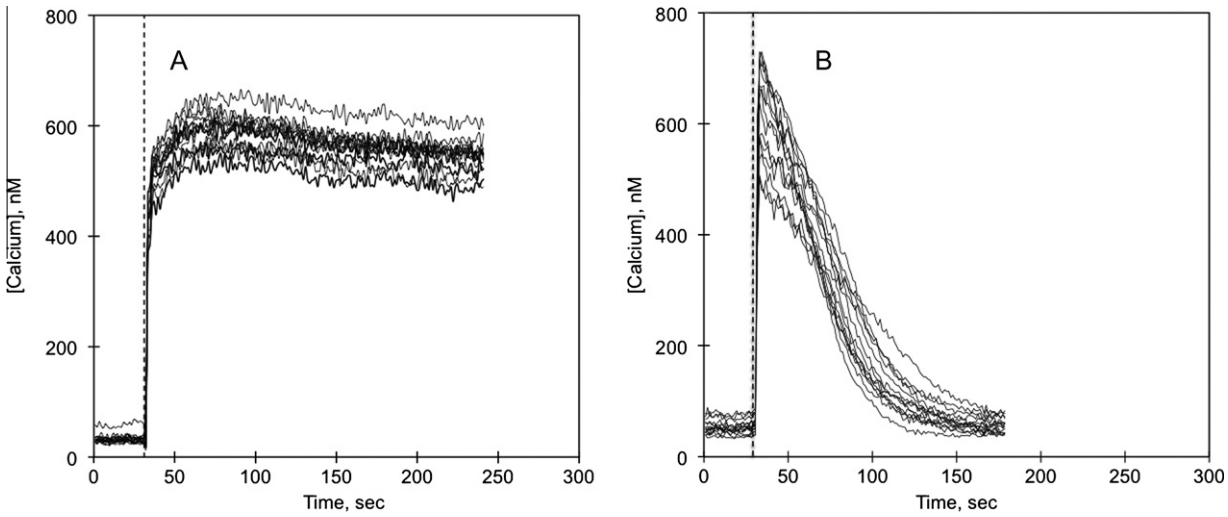


**Fig. 1.** The influence of cholinergic activation on cytosolic calcium levels in CHO-M3 cells. CHO cells stably transfected with the gene for human M3 muscarinic acetylcholine receptor (CHO-M3) were loaded with fura-2AM dye for 40 min at room temperature. The loading dye was removed and replaced with basal salt solution (BSS) and the cells were incubated for an additional 20 min. The BSS solution was replaced by fresh BSS or BSS without calcium immediately before measuring intracellular calcium levels. (**A**) Control responses in the presence of 2 mM extracellular calcium. Carbamylcholine (10 μM) was added at the time indicated by the dashed vertical line. (B) Control responses measured in the absence of extracellular calcium. Each line represents the response of an individual cell from a single experiment. These results are representative of responses from more than 25 independent experiments. The resting calcium level was 38 ± 7 nM ($N$ = 20) in the presence and 57 ± 14 ($N$ = 16) in the absence of extracellular calcium ($p < 0.01$). Two components of the calcium response to extracellular calcium are evident: a rapid response reflecting release from the endoplasmic reticulum and a delayed plateau response dependent on the influx of extracellular calcium.

calcium was not maintained (Fig. 1B). This is consistent with the common interpretation of these measurements: the initial response reflects calcium release from the endoplasmic receptor mediated by the IP3 receptor, while the sustained plateau phase reflects calcium entry from the extracellular medium. The initial phase involves activation of IP3 receptors; the plateau phase reflects "capacitive" calcium entry through Orai channels in response to activation by calcium sensitive STIM1 proteins in the membrane of the endoplasmic reticulum (Bird et al., 2008). This interpretation is further supported by the rapid elimination of the plateau response upon chelation of extracellular calcium with EDTA (not shown). The influx of extracellular calcium in response to depletion of calcium in the endoplasmic reticulum has been termed store-activated calcium entry (SOCE). There was a small but significant increase in cytosolic calcium concentration when calcium was excluded from the extracellular medium (57 ± 14 ($N$ = 20) vs. 38 ± 7 nM ($N$ = 16); $p > 0.01$).

### 3.2. Influence of ZnO nanoparticles on calcium responses mediated by M3 muscarinic receptors

Exposure of CHO-M3 cells to ZnO nanoparticles altered cellular calcium responses to muscarinic receptor stimulation is several ways (Fig. 2). Cells that were incubated for 1 h with a high (50 μg/ml) concentration of ZnO particles had markedly elevated resting calcium concentrations (over 200 nM), although the cells were still able to maintain the calcium concentration at this high level (high and variable intracellular calcium concentrations are associated with damaged and apoptotic cells). Cells exposed to ZnO responded to 10 μM carbamylcholine with an increase in calcium to about 500 nM, however the increase was not sustained, even though 2 mM extracellular calcium was present. The calcium level relaxed to a new, somewhat higher baseline (≈250 nM) within 2 min. Thus, IP3 receptor mediated release from the endoplasmic reticulum appears to be largely intact, while SOCE was selectively blocked.

A more complete dose–response for the effect of ZnO on resting calcium concentration is presented as Fig. 2B, which summarizes the results from multiple experiments. ZnO increased the resting calcium concentration at all concentrations examined (1.5–50 μg/ml); there was a 4.8-fold increase with 50 μg/ml ZnO. The cells were able to maintain a stable resting calcium concentration at all ZnO concentrations.

Responses of CHO-M3 cells to carbamylcholine in the presence of lower (2 and 5 μM) concentrations of ZnO are illustrated in Fig. 3. The signal effect is the failure of the cells to maintain a plateau calcium response to muscarinic stimulation.

### 3.3. Cytotoxicity of ZnO nanoparticles

CHO-M3 cell viability was revealed by the ability of cells to reduce MTS. ZnO induced cytotoxicity in a time and concentration-dependent manner (Fig. 4). The concentration/cytotoxicity curve was remarkably steep following a 24 h exposure to ZnO: Toxicity was minimal at concentrations below 20 μg/ml but virtually complete at ZnO concentrations above 28 μg/ml. More gradual and less complete toxicity was observed with shorter exposure times. It is clear, however, that ZnO has marked effects on resting calcium concentrations and SOCE under conditions of concentration and exposure time that do not cause significant cytotoxicity.

### 3.4. Influence of ZnO nanoparticles on store-operated calcium entry

Thapsigargin is a cell permeable, sesquiterpene alkaloid that inhibits the sarco/endoplasmic reticulum ATPases (SERCA) that transport calcium from the cytosol into the endoplasmic reticulum. Inhibition of SERCAs causes a depletion of calcium from the endoplasmic reticulum and a rise in cytosolic calcium (Rogers et al., 1995). SOCE can be identified by depleting the endoplasmic reticulum with thapsigargin in a calcium-free medium, followed by the reintroduction of extracellular calcium (Bird et al., 2008). Extracellular calcium rapidly enters the cell through SOCE channels previously opened in response to thapsigargin-mediated depletion of endoplasmic reticulum calcium stores.

In CHO-M3 cells incubated in BSS containing 2 mM calcium, thapsigargin elicited a two-phase response, an initial rather slow

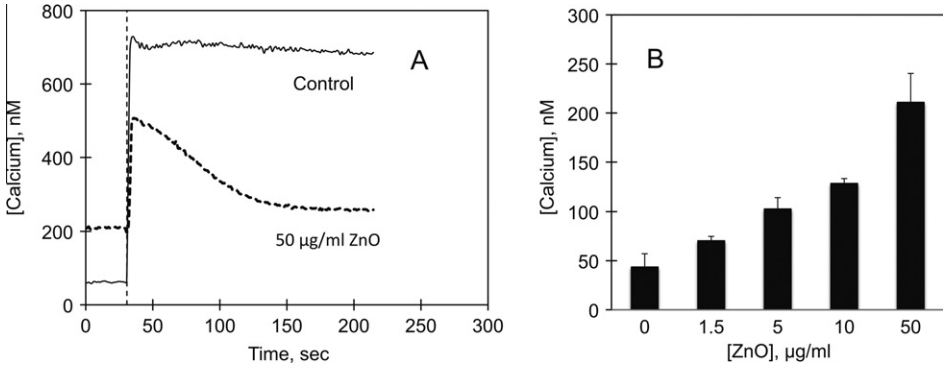


**Fig. 2.** Influence of 50 μg/ml ZnO nanoparticles on cholinergic receptor-mediated changes in cytosolic calcium. Intracellular calcium levels were measured in CHO-M3 cells in the absence (Control) and presence of 50 μg/ml ZnO, as indicated. (**A**) Carbamylcholine was added at the time indicated by the dashed vertical line. The cells were incubated with ZnO in DMEM for 1 h. The DMEM was removed and the cells were loaded with fura-2AM dye in BSS for 1 h. The cells were then rinsed with BSS and incubated for a further 30 min before calcium content was measured. ZnO was continually present in the treated cells during all of these procedures. Three effects of ZnO on the calcium responses were apparent: an increase in resting calcium concentration to >200 nM, a decrease in the phasic initial response and an elimination of the plateau response. (**B**) The influence of ZnO nanoparticles on resting calcium concentration. Each column and bar represents the mean and standard deviation from 3–6 experiments, each including separate measurements from 15–25 cells. The resting calcium concentration in the presence of each ZnO concentration was greater than the concentration in control cells ($p < 0.01$).

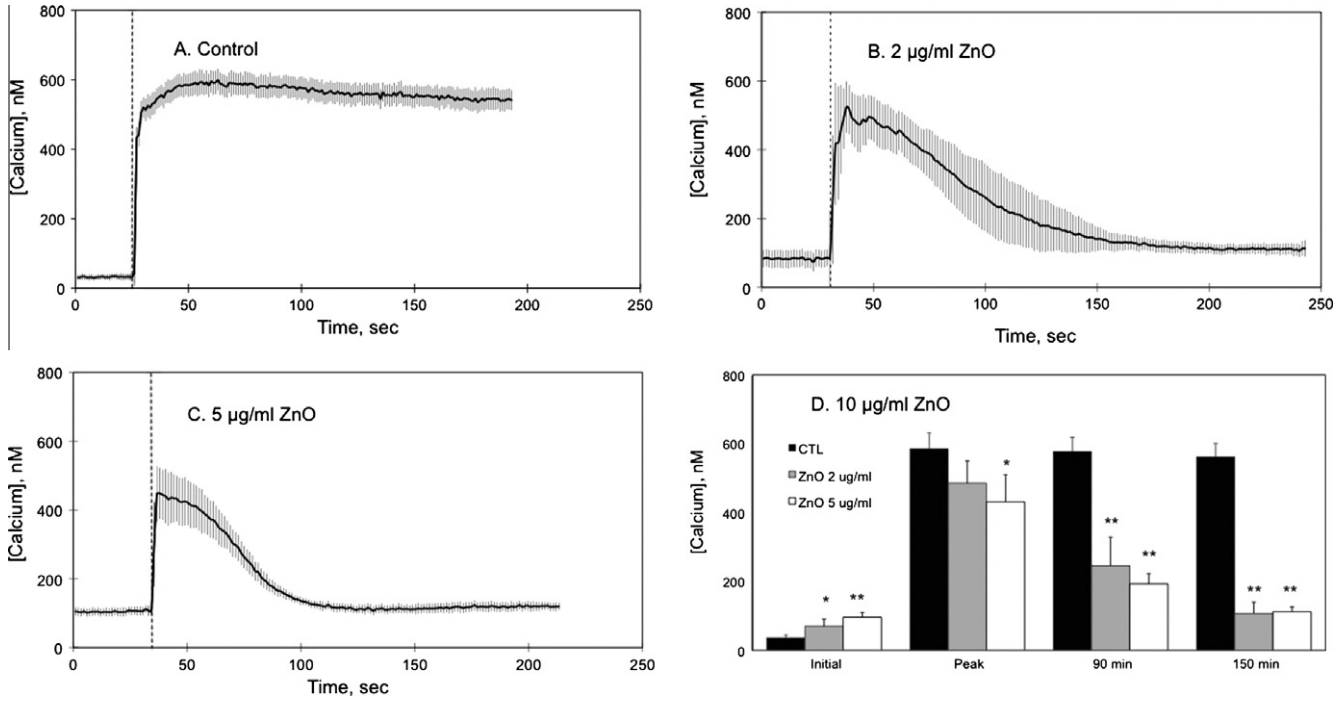


**Fig. 3.** Influence of low concentrations of ZnO nanoparticles on M3 muscarinic receptor-mediated changes in cytosolic calcium in cultured CHO-M3 cells. Responses of CHO-M3 cells to 10 μM carbamylcholine (added at the time indicated by the dashed vertical lines) were measured in the absence and presence of 2 or 5 μg/ml ZnO (Panels **A**, **B** and **C**, as indicated). Cells were pretreated with ZnO for 1 h before loading with fura-2AM, and ZnO was continuously present throughout the experimental protocol. The lines and vertical bars represent the mean and standard deviations from 30–55 cells from three independent experiments. Calcium response values at four time points are presented in Panel **D**. "Initial" denotes resting calcium concentration before addition of carbamylcholine; "Peak" indicates the initial response measured 10 s after the addition of carbamylcholine and reflecting calcium release from the endoplasmic reticulum; "90 min" and "150 min" indicate calcium concentrations measured 90 and 150 s after the addition of carbamylcholine and reflect the ability of the cell to maintain the influx of extracellular calcium. *, $p < 0.05$: different from untreated control cells at that time point; **, $p < 0.01$: different from untreated control cells at that time point.

release followed by a sustained calcium plateau (Fig. 5). The plateau phase was immediately eliminated by addition of 5 mM EDTA to the extracellular medium, indicating its dependence on the influx of extracellular calcium. Exposure of CHO-M3 cells to thapsigargin (1 μM) in a calcium-free medium led to an increase of intracellular calcium to about 260 nM (Fig. 5). Calcium concentration peaked 75 s after thapsigargin addition and returned to baseline within a few minutes. Addition of carbamylcholine after return to the baseline failed to elicit any response (not shown).

Addition of 2 mM calcium following exposure of CHO-M3 cells to thapsigargin (1 μM) in a calcium-free medium resulted in a rapid and persistent increase in calcium concentration to ≈600 nM (Fig. 6A). The influences of ZnO nanoparticles on SOCE measured in CHO-M3 in this manner (i.e., in calcium-free media) are illustrated in Fig. 6B and C. Exposure to 1.5, 5 or 10 μg/ml ZnO produced the previously described concentration-dependent rise in resting cytosolic calcium concentration. Thapsigargin produced a small, slowly developing and transient increase in cellular calcium

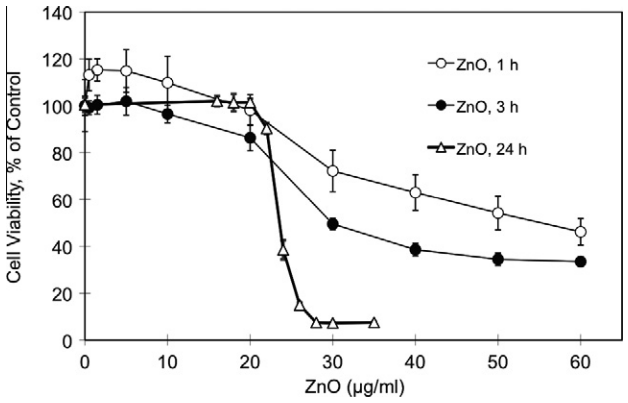


**Fig. 4.** Cytotoxicity of ZnO. CHO-M3 cells were exposed to ZnO nanoparticles at the concentrations indicated on the abscissa for 1, 3 or 24 h, as indicated. Cell viability was then determined using the MTS assay. Points and bars indicate the means and standard deviations from 3 determinations.

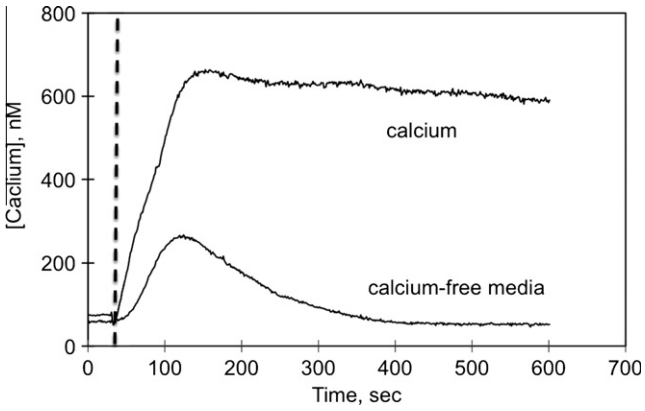


**Fig. 5.** Influence of thapsigargin on cytosolic calcium concentrations in CHO-M3 cells. Thapsigargin (1 μM) was added at the time indicated by the vertical dashed line. Calcium concentration was determined in the absence and presence of extracellular calcium, as indicated. Each line is the average response from 23 cells from a single experiment; eight replicate experiments yielded essentially identical results.

concentration; there was no difference in the maximum calcium concentration attained in response to thapsigargin in the presence of ZnO (1.5–10 μg/ml), although the magnitude of the calcium response differed because of the higher baseline concentration. However, ZnO greatly attenuated the subsequent rise in calcium concentration in response to the addition of extracellular calcium: There was no response in the presence of 10 μg/ml ZnO, and responses were smaller and of shorter duration in cells exposed to 1.5 and 5 μg/ml ZnO (Fig. 6B and C).

### *3.5. Influence of ZnO nanoparticles on muscarinic receptor ligand binding properties*

The possibility that ZnO affected the muscarinic receptor component of this signal transduction pathway was evaluated using a specific radiolabelled probe, [$^3$H]MS. [$^3$H]MS binding was well-described by a binding isotherm for ligand binding to a single population of independent receptors (Fig. 7A; Table 1). Receptor affinity for [$^3$H]MS was high; nonlinear regression analysis revealed a dissociation constant of 1.9 ± 0.2 nM. Binding affinity was not affected by the inclusion of high concentrations of ZnO nanoparticles (10 and 20 μg/ml) in the binding reaction (Table 1). [$^3$H]MS binding was also measured in membranes from CHO-M3 that had been exposed to ZnO nanoparticles (10 and 20 μg/ml) for 5 h before the cells were harvested for binding measurements. Again, there was no effect on [$^3$H]MS binding affinity (Table 1). There was, however, a consistent increase in the concentration of binding sites, expressed as binding sites/total cell protein. A time course for the development of this increase is presented in Fig. 7B. The concentration of sites increased following incubations with 2 μg/ml ZnO for up to 8 h, but decreased with longer exposure times.

Agonist binding to muscarinic receptors reveals certain aspects of receptor organization. Agonist binding was inferred from the ability of carbamylcholine to inhibit the binding of 0.3 M [$^3$H]MS to the receptor (Fig. 8A). Carbamylcholine inhibited [$^3$H]MS binding with a uniformly low affinity (IC50 ≈40 μM); the shape of the isotherm was consistent with binding to a single population of receptors. Inclusion of 5'guanylylimidodiphosphate (Gpp(NH)p; 50 μM) in the incubation medium had a small affect on the ability of carbamylcholine to inhibit [$^3$H]MS binding. ZnO (2 μg/ml) markedly increased carbamylcholine binding affinity, although Gpp(NH)p did not affect carbamylcholine binding in the presence of ZnO (Fig. 8A).

Muscarinic receptors can also be regulated by ligands that bind to an allosteric site. This allosteric effect is clearly evident in a decrease in the rate of [$^3$H]MS dissociation in the presence of the allosteric ligand (e.g., (Stahl and Ellis, 2010)). We measured this dissociation in the presence of a high (20 μg/ml) concentration of ZnO (Fig. 8B). ZnO had no effect on atropine-induced dissociation of an M3-[$^3$H]MS complex in CHO-M3 cells. Moreover, ZnO did not affect the ability of the allosteric ligand gallamine to slow the rate of dissociation (Fig. 8B; Table 1).

## 4. Discussion

The goal of this research was to determine the effects of ZnO nanoparticles on muscarinic signaling. CHO cells are widely used in the study of muscarinic pathways. CHO cells do not natively express muscarinic receptors or acetylcholinesterase, but express elements of phospholipase Cβ and adenylate cyclase signaling pathways. Moreover, CHO cells transfected with transgenes for the different muscarinic receptor subtypes respond to muscarinic agonists in pharmacologically and physiologically appropriate fashions.

A wide variety of metal oxide nanoparticles are toxic to cultured cells, producing oxidative stress that induces apoptosis (Huang et al., 2009). In the present study, ZnO nanoparticles induced cytotoxicity in CHO cells in a concentration and time dependent fashion. However, inhibitory effects of nanoparticles on muscarinic signaling and SOCE could be detected under conditions that did not produce overt cytotoxicity.

The present results demonstrate some specific effects of ZnO particles on early aspects of M3 receptor activation. Receptor binding of the antagonist [$^3$H]MS was not affected, nor were allosteric ligand effects on receptor binding. Interestingly, ZnO nanoparticles markedly enhanced the ability of carbamylcholine to inhibit [$^3$H]MS binding, and this increase was not affected by inclusion of a guanine nucleotide in the incubation medium. Such effects have been previously associated with metals and protein oxidants (Aronstam et al., 1978; Aronstam and Eldefrawi, 1979). The functional significance of this shift is problematic, however, since downstream signaling (e.g., IP3 receptor-mediated calcium release from the ER) remained intact. It should be noted, however, that ligand binding to M3 receptors expressed in model systems is much less sensitive to both guanine nucleotides and allosteric agents than either M2 or M4 muscarinic receptors. A determination of the effects of ZnO on these receptor subtypes is presently underway.

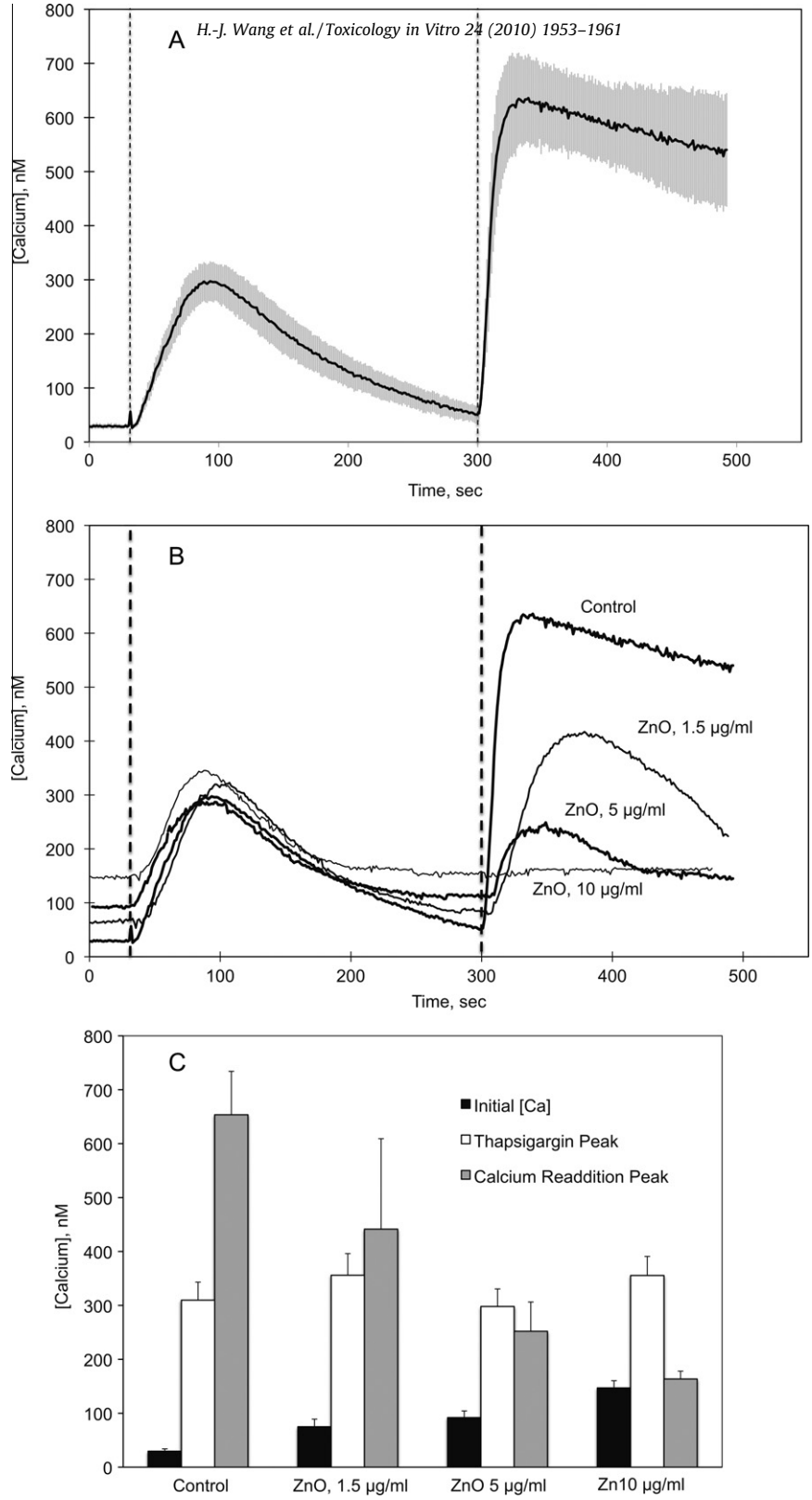


**Fig. 6.** Influence of ZnO on store-operated calcium entry experimentally isolated by exposure to thapsigargin in the absence of extracellular calcium, followed by the reintroduction of calcium. **Panel A**: CHO-M3 cells incubated in the BSS not containing calcium were exposed to thapsigargin (1 μM) at the time indicated by the first dashed vertical line. Calcium was added to the external medium at the time indicated by the second dashed vertical line to a final concentration of 2 mM. The increase in cytosolic calcium concentration caused by the reintroduction of calcium in ER calcium-depleted cells reflects the capacitive store-operated calcium entry (SOCE) (Bird et al., 2008). **Panel B**: CHO-M3 cell were incubated in the absence or presence of 1.5, 5 or 10 μg/ml ZnO nanoparticles for 1.5 h before being loaded with fura-2AM for calcium measurements. Thapsigargin (1 μM) and calcium (2 mM) were added sequentially at the times indicated by the dashed vertical lines. Each line represents the mean from 15–24 cells from a typical experiment; three identical experiments yielded essentially similar results. **Panel C**: Summary of ZnO influences on store-operated calcium entry. Each bar represents the mean and standard deviation from 3 experiments performed as indicated in Panel B. Cells were untreated (Control) or exposed to 1.5, 5 or 10 μg/ml ZnO, as indicated, for 1.5 h before being loaded with fura-2Am for measurement of intracellular calcium. The 3 columns indicate the calcium concentrations before (“Initial”) addition of thapsigargin, at the maximum response realized within 100 s of the addition of thapsigargin (“Thapsigargin Peak”), or the maximum response achieved within 100 s of raising the extracellular calcium concentration to 2 mM (“Calcium Readdition Peak”). Resting calcium concentrations in the presence of all ZnO concentrations were different from the control level ($p < 0.01$). ZnO did not affect the “Thapsigargin Peak” calcium concentrations; the “Calcium Readdition Peak” concentrations were lower in the presence of 5 and 10 μg/ml ZnO ($p < 0.01$).

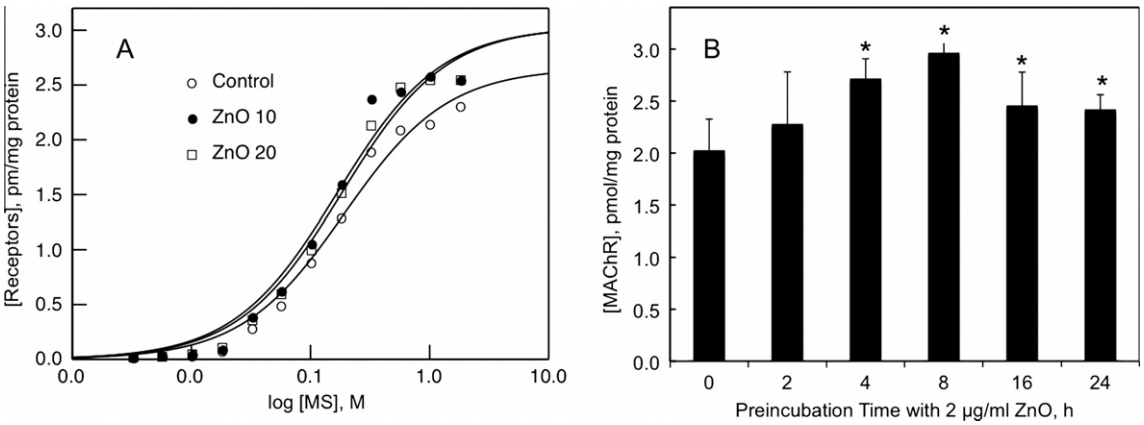


**Fig. 7.** Influence of ZnO nanoparticles on antagonist binding to muscarinic receptors in CHO-M3 cells. **Panel A**. The specific binding of [$^3$H]*N*-methylscopolamine ([$^3$H]MS) was measured at the concentrations indicated on the abscissa. The curve is drawn according to parameters derived from a nonlinear fit of the data to a model for ligand binding to a single population of independent receptors. Each data point reflects the mean from three experiments performed in triplicate. Binding parameters and experimental variation are presented in Table 1. An increase in the receptor concentration was a consistent observation. This increase was a function of time of exposure to ZnO, as shown for 2 µg/ml ZnO in **Panel B**. Each bar represents the receptor concentration in CHO-M3 cells determined by nonlinear regression on data from three experiments. *, $p < 0.05$: different from no preincubation control cells.

**Table 1**
Parameters associated with [$^3$H]MS binding to M3 receptors expressed in CHO cells.

| Cell treatment | $K_D$ (nM) | [Receptor] (pmol/mg protein) | $k_{-1}$ | $k_{-1}$ (Gallamine) |
|---|---|---|---|---|
| Control | 1.92 ± 0.2 | 2.65 ± 0.3 | 0.021 ± 0.005 | 0.006 ± 0.002 |
| ZnO 10 µg/ml | 1.67 ± 0.3 | 3.03 ± 0.2 | | |
| ZnO 10 µg/ml, 5 h | 1.98 ± 0.4 | 2.93 ± 0.4 | 0.024 ± 0.008 | 0.007 ± 0.002 |
| ZnO 20 µg/ml | 1.83 ± 0.4 | 3.03 ± 0.3 | | |
| ZnO 20 µg/ml, 5 h | 1.60 ± 0.3 | 2.82 ± 0.4 | | |

[$^3$H]MS binding was measured in untreated cells (Control) or in cells exposed to ZnO acutely or for 5 h before harvesting the cells for binding measurements, as indicated. Gallamine is a potent allosteric modulator that decreases ligand dissociation; it is included as a positive control.
$K_D$, dissociation constant; [Receptor], receptor density.
$k_{-1}$, Rate constant of dissociation, $s^{-1}$, measured in the absence and presence of 10 µM gallamine, as indicated. Gallamine decreased the dissociation rate constants ($p < 0.01$); the rate constants were not altered in the presence of 10 µg/ml ZnO.
Mean ± SD ($N = 3$). None of the parameters measured in the presence of ZnO were significantly different from the corresponding control value.

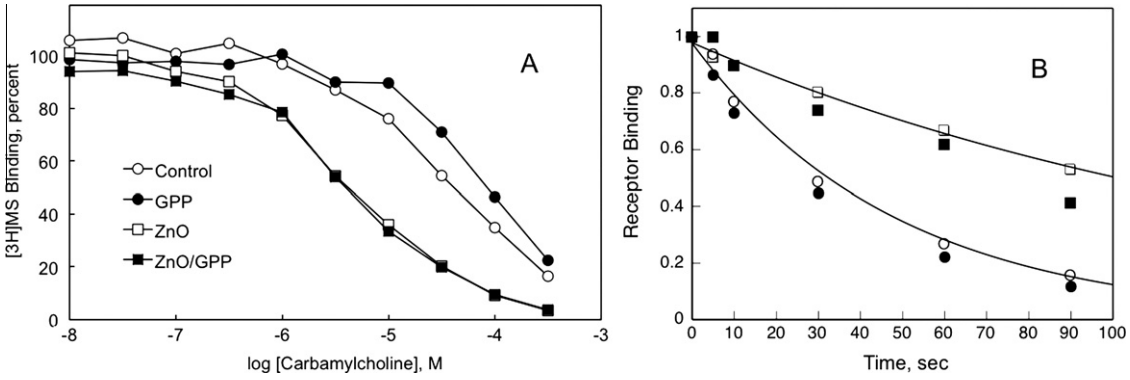


**Fig. 8.** Influence of ZnO nanoparticles on agonist binding to M3 muscarinic receptors expressed by CHO cells. **Panel A**. The ability of carbamylcholine to inhibit the specific binding of 0.3 nM [$^3$H]MS was determined in triplicate in the absence (circles) or presence (squares) of 2 µg/ml ZnO in the absence (open symbols) or presence (closed symbols) of 10 µM Gpp(NH)p. Each point is the average of three measurements from three independent experiments. Carbamylcholine inhibition of [$^3$H]MS binding was mitigated in the presence of 5′-Gpp(NH)p (IC50′s = 48 ± 6 and 100 ± 19 in the absence and presence of 5′-Gpp(NH)p, respectively; $p < 0.01$). Carbamylcholine inhibition of [$^3$H]MS binding was greatly enhanced in the presence of ZnO (IC50 = 4.5 ± 0.4; $p < 0.01$), but this inhibition was no longer sensitive to 5′-Gpp(NH)p (IC50 = 4.5 ± 0.3). **Panel B**. The influence of ZnO nanoparticles on allosteric regulation of M3 muscarinic receptors expressed in CHO cells is illustrated. The dissociation of [$^3$H]MS was measured by incubating CHO-M3 cell membranes with 1 nM [$^3$H]MS for 1 h before adding an excess of atropine (10 µM) to block the forward reaction. The off rate was measured in the absence (circles) and presence (squares) of 10 µM gallamine in the absence (open symbols) and presence (closed symbols) of 10 µg/ml ZnO. Dissociation rate constants are listed in Table 1.

ZnO had a paradoxical positive effect on the concentration of M3 binding sites. It is possible that the cytotoxic effects of ZnO particles preferentially affect the expression of cellular proteins with high turn over rates, thereby increasing M3 concentration expressed on the basis of cellular protein (muscarinic receptors, and many membrane proteins, have relatively long half lives (e.g., (Haddad et al., 1995)). An alternate explanation is that oxidative stress increased expression controlled by the cytomegalovirus

promoter that is upstream of the M3 coding region (Bruening et al., 1998).

ZnO particles had two prominent effects on the IP3 signaling pathway activated by M3 activation: an increase in resting calcium concentration and a potent inhibition of the SOCE. ZnO increased resting $[Ca^{2+}]_i$ from 40 to 130 nM when present in noncytotoxic concentrations from 1.5 to 10 μg/ml. The cells were capable of maintaining $[Ca^{2+}]_i$ at the new, higher $[Ca^{2+}]_i$ for at least an hour. The basis for this increase is not clear, but may involve impairment of the active transport processes or ion exchange mechanisms that determine calcium concentration (Ermak and Davies, 2002).

ZnO particles did not affect calcium release from the ER caused by thapsigargin inhibition of the $Ca^{2+}$-ATPases that transport calcium from the cytosol to the lumen of the ER. The maximal cytosolic calcium concentrations produced by exposure to thapsigargin were not affected by ZnO particles, however, since the resting $[Ca^{2+}]_i$ was higher in the presence of ZnO, the absolute magnitude of the response was lower. After a few minutes, the cells reverted to the resting $[Ca^{2+}]_I$ associated with that particular concentration of ZnO, i.e., homeostatic mechanisms maintained $[Ca^{2+}]_{at}$ at the new baseline level. This suggests that the rise in resting $[Ca^{2+}]_I$ in the presence of ZnO does not involve a change in $Ca^{2+}$-ATPases that are susceptible to thapsigargin (i.e., SERCAs).

The most prominent effect of ZnO particle on the muscarinic receptor–IP3 signaling pathway was a selective inhibition of the store-operated calcium entry (SOCE) that is activated by the depletion of calcium from the endoplasmic reticulum. The molecular details of this classic pathway have recently been described in detail (e.g., (Putney, 2009)). This effect is manifested as a decrease in the plateau phase of the response that is dependent on the entry of extracellular calcium (Fig. 3), as well as in a calcium readdition paradigm following depletion of endoplasmic stores. The concentration dependence for both effects is the same (EC50 ≈ 2 μg/ml).

ZnO particles had a small effect on the initial rise in $[Ca^{2+}]_I$ to carbamylcholine that reflects calcium release from the endoplasmic reticulum through activated IP3 receptor $Ca^{2+}$ channels. For example, the initial peak was reduced 20% by a ZnO concentration (5 μg/ml) that totally eliminated SOCE within 60 s. At even the highest ZnO concentrations tested (50 μg/ml), IP3 receptor-mediated calcium release was not decreased by more than 30%. The contribution of the increased resting $[Ca^{2+}]_I$ on the decrease in magnitude of the IP3 receptor-mediated calcium release is not clear.

The aspect of the ZnO nanoparticles responsible for these effects is being studied utilizing particles of different size and surface area. Zinc metal ions have multiple and profound effects on ion channel functions (and muscarinic receptors, e.g., (Aronstam et al., 1978)), however, ICP-MS analysis revealed little dissolution of zinc from the particles under the present experimental conditions (Huang et al. unpublished observations). The extent to which the ZnO effects can be ascribed to oxidative stress requires further study.

Thus, the present results demonstrate a specific inhibitory effect of ZnO nanoparticles on the M3 muscarinic–phospholipase Cβ signaling pathway: ZnO particles selectively inhibit store-operated calcium entry. ZnO particles also change the resting $[Ca^{2+}]_i$ without compromising the homeostatic mechanisms that maintain cytosolic calcium concentrations at low levels. The effects of ZnO particles on this pathway are specific insofar as receptor antagonist binding, allosteric muscarinic receptor effects, and IP3 receptor binding and activation are not greatly perturbed.

## Acknowledgment

This work was supported by the Missouri S&T cDNA Resource Center.

## References

Aronstam, R.S., Abood, L.G., Hoss, W., 1978. Influence of sulfhydryl reagents and heavy metals on the functional state of the muscarinic acetylcholine receptor in rat brain. Mol. Pharmacol. 14, 575–586.

Aronstam, R.S., Eldefrawi, M.E., 1979. Reversible conversion between affinity states for agonists of the muscarinic acetylcholine receptor from rat brain. Biochem. Pharmacol. 28, 701–703.

Aronstam, R.S., Patil, P., 2009. Muscarinic receptors: autonomic neurons. In: Squire, L.R. (Ed.), Encyclopedia of Neuroscience, fourth ed. Academic Press, Oxford, pp. 1141–1149.

Bae, S.Y., Seo, H.W., 2004. Vertically aligned sulfur-doped ZnO nanowires synthesized via chemical vapor deposition. J. Phys. Chem. 108, 5206–5210.

Bai, X.D., Gao, P.X., Wang, Z.L., Wang, E.G., 2003. Al-mode mechanical resonance of individual ZnO nanobelts. Appl. Phys. Lett. 28, 4806–4808.

Beckett, W.S., Chalupa, D.F., Pauly-Brown, A., Speers, D.M., Stewart, J.C., Frampton, M.W., Utell, M.J., Huang, L.S., Cox, C., Zareba, W., Oberdorster, G., 2005. Comparing inhaled ultrafine versus fine zinc oxide particles in healthy adults: a human inhalation study. Am. J. Respir. Crit. Care Med. 171, 1129–1135.

Bird, G.S., DeHaven, W.I., Smyth, J.T., Putney Jr., J.W., 2008. Methods for studying store-operated calcium entry. Methods 46, 204–212.

Braydich-Stolle, L., Hussain, S., Schlager, J.J., Hofmann, M.C., 2005. In vitro cytotoxicity of nanoparticles in mammalian germline stem cells. Toxicol. Sci. 88, 412–419.

Bruening, W., Giasson, B., Mushynski, W., Durham, H.D., 1998. Activation of stress-activated MAP protein kinases up-regulates expression of transgenes driven by the cytomegalovirus immediate/early promoter. Nucleic Acids Res. 26, 486–489.

Calderon-Garciduenas, L., Azzarelli, B., Acuna, H., Garcia, R., Gambling, T.M., Osnaya, N., Monroy, S., Del Tizapantzi, M.R., Carson, J.L., Villarreal-Calderon, A., Rewcastle, B., 2002. Air pollution and brain damage. Toxicol. Pathol. 30, 373–389.

Calderon-Garciduenas, L., Valencia-Salazar, G., Rodriguez-Alcaraz, A., Gambling, T.M., Garcia, R., Osnaya, N., Villarreal-Calderon, A., Devlin, R.B., Carson, J.L., 2001. Ultrastructural nasal pathology in children chronically and sequentially exposed to air pollutants. Am. J. Respir. Cell Mol. Biol. 24, 132–138.

Comini, E., Faglia, G., Sberveglieri, G., Pan, Z., Wang, Z.L., 2002. Stable and highly sensitive gas sensors based on semiconducting oxide nanobelts. Appl. Phys. Lett. 81, 1869–1871.

Ding, Y., Wang, Z.L., 2004. Structure analysis of nanowires and nanobelts by transmission electron microscopy. J. Phys. Chem. 108, 12280–12291.

Elder, A., Gelein, R., Silva, V., Feikert, T., Opanashuk, L., Carter, J., Potter, R., Maynard, A., Ito, Y., Finkelstein, J., Oberdorster, G., 2006. Translocation of inhaled ultrafine manganese oxide particles to the central nervous system. Environ. Health Perspect. 114, 1172–1178.

Ermak, G., Davies, K.J., 2002. Calcium and oxidative stress: from cell signaling to cell death. Mol. Immunol. 38, 713–721.

Fine, J.M., Gordon, T., Chen, L.C., Kinney, P., Falcone, G., Beckett, W.S., 1997. Metal fume fever: characterization of clinical and plasma IL-6 responses in controlled human exposures to zinc oxide fume at and below the threshold limit value. J. Occup. Environ. Med. 39, 722–726.

Gurr, J.R., Wang, A.S., Chen, C.H., Jan, K.Y., 2005. Ultrafine titanium dioxide particles in the absence of photoactivation can induce oxidative damage to human bronchial epithelial cells. Toxicology 213, 66–73.

Haddad, E.B., Rousell, J., Barnes, P.J., 1995. Muscarinic M2 receptor synthesis: study of receptor turnover with propylbenzilylcholine mustard. Eur. J. Pharmacol. 290, 201–205.

Huang, C.C., Aronstam, R.S., Chen, D.R., Huang, Y.W., 2009. Oxidative stress, calcium homeostasis, and altered gene expression in human lung epithelial cells exposed to ZnO nanoparticles. Toxicol. In Vitro.

Huang, G.G., Wang, C.T., Tang, H.T., Huang, Y.S., Yang, J., 2006. ZnO nanoparticle-modified infrared internal reflection elements for selective detection of volatile organic compounds. Anal. Chem. 78, 2397–2404.

Jeng, H.A., Swanson, J., 2006. Toxicity of metal oxide nanoparticles in mammalian cells. J. Environ. Sci. Health A Toxicol. Hazard Subst. Environ. Eng. 41, 2699–2711.

Lewinski, N., Colvin, V., Drezek, R., 2008. Cytotoxicity of nanoparticles. Small 4, 26–49.

Lin, W., Huang, Y.W., Zhou, X.D., Ma, Y., 2006a. In vitro toxicity of silica nanoparticles in human lung cancer cells. Toxicol. Appl. Pharmacol. 217, 252–259.

Lin, W., Huang, Y.W., Zhou, X.D., Ma, Y., 2006b. Toxicity of cerium oxide nanoparticles in human lung cancer cells. Int. J. Toxicol. 25, 451–457.

Lin, W., Staytom, I., Huang, Y.W., Zhou, X.D., Ma, Y., 2008. Cytotoxicity and cell membrane depolarization induced by aluminum oxide nanoparticles in human lung epithelial cells A549. Toxicol. Environ. Chem. 90, 983–996.

Moller, W., Brown, D.M., Kreyling, W.G., Stone, V., 2005. Ultrafine particles cause cytoskeletal dysfunctions in macrophages: role of intracellular calcium. Part Fibre Toxicol. 2, 7.

Putney, J.W., 2009. Capacitative calcium entry: from concept to molecules. Immunol. Rev. 231, 10–22.

Ramakrishna, G., HGhosh, H.N., 2003. Effect of particle size on the reactivity of quantum size ZnO nanoparticles and charge-transfer dynamics with adsorbed catechols. Langmuir 19, 3606–3612.

Rogers, T.B., Inesi, G., Wade, R., Lederer, W.J., 1995. Use of thapsigargin to study $Ca2^+$ homeostasis in cardiac cells. Biosci. Rep. 15, 341–349.

Sharma, H.S., Sharma, A., 2007. Nanoparticles aggravate heat stress induced cognitive deficits, blood–brain barrier disruption, edema formation and brain pathology. Prog. Brain Res. 162, 245–273.

Smyth, J.T., Dehaven, W.I., Bird, G.S., Putney Jr., J.W., 2008. $Ca2^{+}$-store-dependent and -independent reversal of Stim1 localization and function. J. Cell Sci. 121, 762–772.

Stahl, E., Ellis, J., 2010. Novel allosteric effects of amiodarone at the muscarinic M5 receptor. J. Pharmacol. Exp. Ther.

Timblin, C.R., Shukla, A., Berlanger, I., BeruBe, K.A., Churg, A., Mossman, B.T., 2002. Ultrafine airborne particles cause increases in protooncogene expression and proliferation in alveolar epithelial cells. Toxicol. Appl. Pharmacol. 179, 98–104.

Veronesi, B., Makwana, O., Pooler, M., Chen, L.C., 2005. Effects of subchronic exposures to concentrated ambient particles. VII. Degeneration of dopaminergic neurons in Apo E−/− mice. Inhal. Toxicol. 17, 235–241.

Zhu, B.L., Xie, C.S., Zeng, Z.W., Song, W.L., Wang, A.H., 2005. Investigation of gas sensitivity of Sb-doped ZnO nanoparticles. Mater. Chem. Phys. 89, 148–153.